Spectrum of three-wave mixing for multimode fields

Y. B. Band, D. F. Heller, and J. S. Krasinski
Allied-Signal Inc., Corporate Technology Center, P.O. Box 1021R, Morristown, New Jersey 07960
*and Ben Gurion University, Beer Sheva, Israel**
(Received 15 February 1989)

Analytic solutions are developed for the time-dependent intensity that results from the three-wave mixing of multimode fields. These differ dramatically from the solutions for single-mode (time-independent) fields. New frequencies in the output spectrum are created as input intensities increase. Under conditions of strong nonlinear coupling the output spectrum broadens, ultimately reaching the phase-match bandwidth limit, and the dynamics can become chaotic. A new technique for enhancing mixing efficiencies is presented.

Three-wave mixing (3WM) processes, second-harmonic generation (SHG), sum-frequency generation (SFG), difference-frequency generation (DFG), and optical parametric oscillation are routinely employed to generate new frequencies from fixed-frequency and tunable-laser sources. The basic physics of 3WM processes has been well understood for over 25 years and analytic solutions have been derived for the mixing of plane-wave, single-mode fields.[1-3] In this article we consider the dynamics of 3WM processes involving multitemporal mode time-dependent fields appropriate to the description of 3WM of typical laser beams. While previous studies have dealt with the spectral consequences of 3WM in the weak-field limit,[4] here we show that analytic expressions are easy to derive for the 3WM of fields of arbitrary strength. Specifically, we show that the spectrum of the output fields generated using SFG, DFG, and SHG changes in a nontrivial manner under conditions of strong coupling. The output spectrum for SFG and DFG can be dense and broad, even for input beams containing only two modes. For large nonlinear coupling the output spectrum broadens, becoming quasicontinuous and exhibiting a bandwidth that approaches the phase-match bandwidth of the nonlinear medium. In contrast, the SHG spectrum remains discrete for an input beam containing only two modes, but its spectral bandwidth can still broaden to the phase-match limit. We present a new technique for enhancing mixing efficiencies based upon the concepts developed here.

The dynamical equations governing SFG of phase-matched plane waves (the DFG equations are similar) are given in the slowly varying envelope approximation by

$$\frac{\partial E_1(z,\tau)}{\partial z} = -i\omega_1\chi E_3 E_2^* ,$$
$$\frac{\partial E_2(z,\tau)}{\partial z} = -i\omega_2\chi E_3 E_1^* , \tag{1}$$
$$\frac{\partial E_3(z,\tau)}{\partial z} = -i\omega_3\chi E_1 E_2 ,$$

where E_1, E_2, and E_3 are the complex interacting electric field envelopes, ω_1, ω_2, and $\omega_3=\omega_1+\omega_2$ are their frequencies, τ is the local pulse time, $\tau=t-x/c$, z is the distance in the medium, $z=x$, and χ is the nonlinear polarization coefficient for the three-wave mixing. Analytic solutions for the intensity (normalized to the absolute square of the electric field) of these fields for real χ are

$$I_3(z,\tau)=\frac{\omega_3}{\omega_{\min}} I_{\min}(0,\tau)\,\mathrm{sn}^2\left[\sqrt{I_{\max}(0,\tau)}\,\omega_{\max}\chi z,\left[\frac{\omega_{\min} I_{\max}(0,\tau)}{\omega_{\max} I_{\min}(0,\tau)}\right]^{1/2}\right],$$
$$I_1(z,\tau)=I_1(0,\tau)-\frac{\omega_1}{\omega_3}I_3(z,\tau),\quad I_2(z,\tau)=I_2(0,\tau)-\frac{\omega_2}{\omega_3}I_3(z,\tau) . \tag{2}$$

Here $\mathrm{sn}(\cdot,\cdot)$ is the doubly periodic Jacobi elliptic function,[5] $I_{\min}(0,\tau)$ [$I_{\max}(0,\tau)$] is the smaller [larger] of the input fields, $I_1(0,\tau)$ and $I_2(0,\tau)$, incident upon the sample at time τ. These solutions are appropriate even when fields 1 and 2 are multifrequency beams. We consider the case where each field (1 and 2) originates from a laser emitting light at several cavity mode frequencies. The temporal dependence of the input fields can then be written as

$$E_i(0,\tau)=\sum_{j=0}^{n} E_{i,j}\sin(\omega_{i,j}\tau+\phi_{i,j}) \quad \text{for } i=1,2 , \tag{3}$$

where $\omega_{i,j}=\omega_i+\Delta_i j$, Δ_i is the mode-frequency spacing of cavity i ($=2\pi c/L_i$, where L_i is the round trip optical length of the ith cavity), and ϕ_{ij} are arbitrary phase shifts for the different modes. The 3WM solution, Eq. (2), is valid provided the spectrum of the fields 1 and 2 remains within the phase-matching bandwidth throughout the

propagation in the crystal and the input envelopes, $E_1(0,\tau)$ and $E_2(0,\tau)$ are real. As we shall see, the output spectrum can be much wider than the set of frequencies $\omega_{3,j,j'}=\omega_{1,j}+\omega_{2,j'}=\omega_1+\omega_2+\Delta_1 j+\Delta_2 j'$, where j and j' are positive or negative integers. We explicitly consider the case of SFG when the input beams contain two axial modes, i.e., $n=1$ in Eq. 3, and Δ_1 and Δ_2 are commensurate and incommensurate (Δ_1/Δ_2 is irrational).

First we consider the more general case of incommensurate frequencies, and we take $\Delta_1=\Delta_0$, $\Delta_2=(8/3\pi)\Delta_0$, ($\Delta_0=1\times10^{10}$ rad/s) and equal field strengths $E_{i,j}$ and equal phases $\phi_{i,j}$ for all field components. We define the (dimensionless) coupling strength parameter u as $u\equiv\{\text{supremum}_\tau[I_{\max}(0,\tau)]\}^{1/2}\omega_{\max}\chi L$, where L is the crystal length (u is the supremum of the first argument of the sn function). In what follows we designate very low, low, medium, and high coupling strengths as follows: $u=8.8\times10^{-3}$, 8.8×10^{-2}, 0.88, and 8.8, respectively. Figure 1 shows the temporal dependence of the output at frequencies ω_1, ω_2, and $\omega_3=\omega_1+\omega_2$ after propagation through a nonlinear mixing crystal at low coupling strength. The input and output intensities at ω_1 and ω_2 are indistinguishable since the conversion is low. The temporal dependence of the intensity at ω_3 reflects the fact that both $I_1(\tau)$ and $I_2(\tau)$ must be large for $I_3(\tau)$ to be large. Figure 2 is similar to Fig. 1, but for intermediate coupling strength. Here, depletion of the input is clear. Figure 3 is for high coupling strength. Sharp temporal features originate from reconversion of $I_3(\tau)$ back into $I_1(\tau)$ and $I_2(\tau)$, and vice versa. When the weaker of $I_1(\tau)$ and $I_2(\tau)$ is fully depleted, $I_3(\tau)$ and the remaining intensity of the stronger of the input fields mix and reform the weaker input field [the output intensity $I_3(z,\tau)$ of Eq. (2) is periodic in the first argument of the sn function provided the second argument is less than unity].

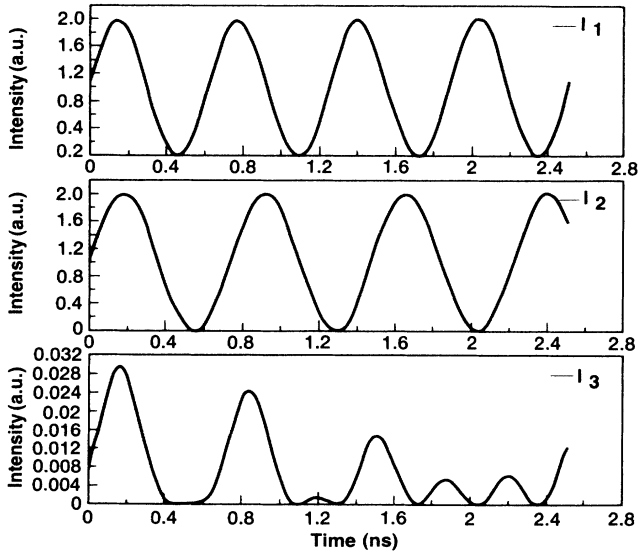

FIG. 1. Time dependence of the output $I_1(\tau)$, $I_2(\tau)$, and $I_3(\tau)$ for incommensurate frequencies Δ_1 and Δ_2 and for low coupling strength. Intensities I_1, I_2, and I_3 are in the same units.

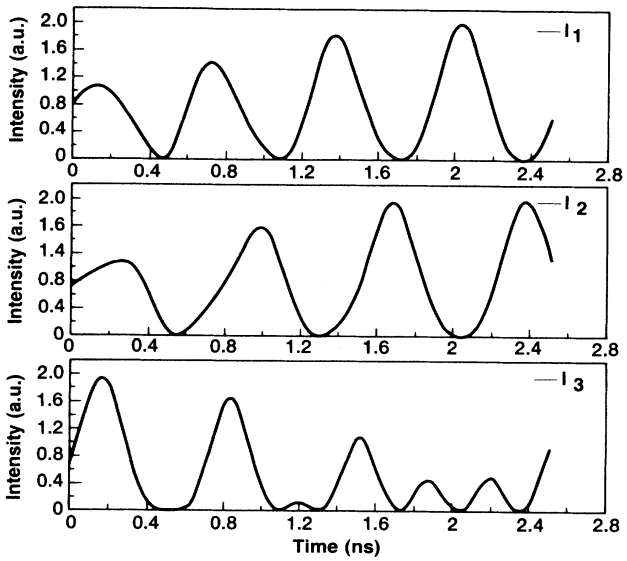

FIG. 2. Same as Fig. 1 but for medium coupling strength.

Thus, when the first argument of sn, proportional to the larger of the input fields, is large and varies with time, the spiky features in Fig. 3 result.

Figure 4 shows the Fourier transform of the output intensity near frequency ω_3 (i.e., the power spectrum of the output intensity) at different coupling strengths. Zero frequency in Fig. 4 corresponds to output at frequency $\omega_1+\omega_2$, and frequency ω corresponds to output at frequencies $\omega_1+\omega_2\pm\omega$. At very low and low coupling strengths the spectrum consists of frequencies 0, $\Delta_1-\Delta_2$, Δ_1 Δ_2, and $\Delta_1+\Delta_2$. The largest components are at frequencies 0, Δ_1, and Δ_2, with the magnitude of the components at $\Delta_1-\Delta_2$, and $\Delta_1+\Delta_2$ much weaker. At intermediate and strong coupling strengths additional frequency components become significant. The spectrum fills in completely, i.e., there is no smallest nonzero frequency in the power spectrum. Despite the chaotic-

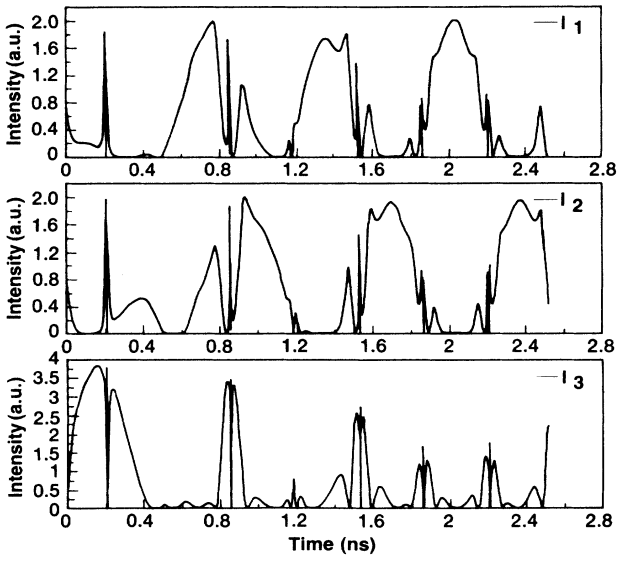

FIG. 3. Same as Fig. 1 but for high coupling strength.

appearing power spectrum for strong coupling strengths, this dynamics are, in fact, not chaotic. However, if phase diffusion is present in the input fields, the dynamics will be chaotic for strong coupling strengths.

We now consider the case of commensurate frequencies Δ_1 and Δ_2. We take $\Delta_1=\Delta_0$, $\Delta_2=(8/9)\Delta_0$, and equal field strengths $E_{i,j}$. Figure 5 shows the temporal dependence of output at frequencies ω_1,ω_2, and $\omega_3=\omega_1+\omega_2$ after propagation through a mixing crystal for low coupling strength. The periodicity (with period $9\times 2\pi/\Delta_0\sim 5.65$ ns) is evident. The output $I_3(\tau)$ is similar to that in Fig. 1 [$(8/3\pi)\Delta_0$ is similar to $(8/9)\Delta_0$], but differences can be seen. Figure 6 shows the power spectrum of the output intensity for very low, low, medium, and high coupling strength. Now, the smallest nonzero frequency in the power spectrum is Δ_0.

The degenerate case, second-harmonic generation, has significantly different properties. The solution of the dynamical equations is

$$I_3(z,\tau)=I_1(0,\tau)\tanh^2[\sqrt{I_1(0,\tau)}\omega_1\chi z]\ ,$$

$$I_1(z,\tau)=I_1(0,\tau)-I_3(z,\tau)\ .$$

In this case, no reconversion from I_3 back to I_1 can occur (the second argument of the sn function equals unity). The power in the higher-order harmonics is less than that for SFG, and the conversion efficiency is higher than in the SFG case (see next paragraph). SHG from a fundamental beam containing frequencies ω_1 and $\omega_1+\Delta$ would contain the three frequencies in the second-harmonic output at low conversion, $2\omega_1$, $2\omega_1+\Delta$, and $2\omega_1+2\Delta$, but for higher coupling strengths, the magnitudes of the higher harmonics $2\omega_1+m\Delta$ grow.

From Figs. 1–3 (and Fig. 4) we can understand that the conversion efficiency of SFG or DFG with multimode beams in significantly less than SHG with multimode

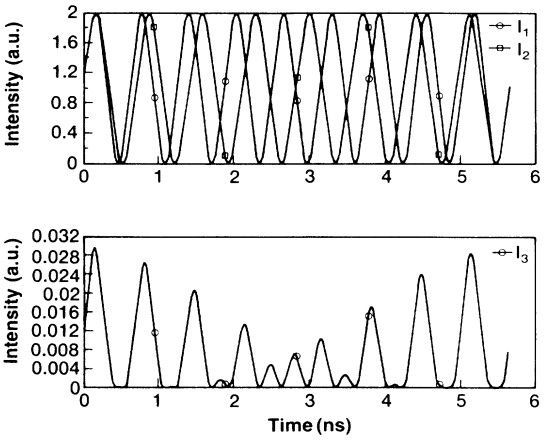

FIG. 5. Same as Fig. 1 but for commensurate frequencies Δ_1 and Δ_2.

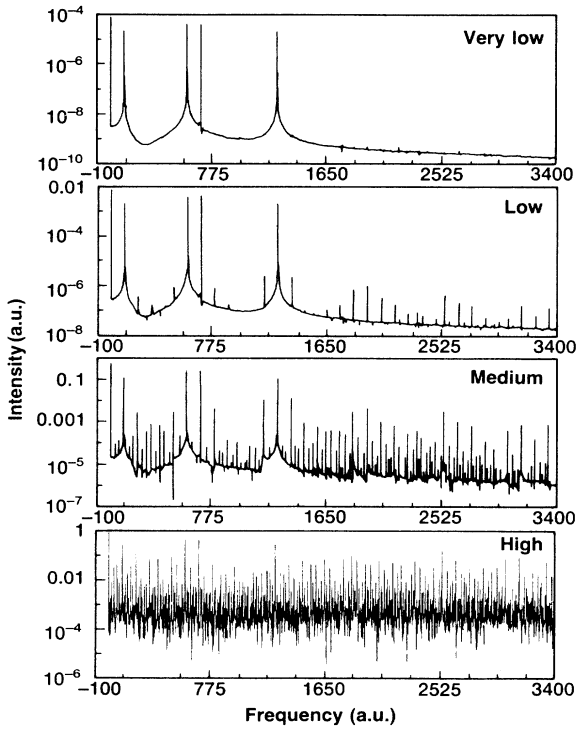

FIG. 4. Power spectrum of the intensity $I_3(\tau)$ for very low, low, medium, and high coupling strength for incommensurate frequencies Δ_1 and Δ_2. The conversion to units of angular frequency is 1 a.u. $\leftrightarrow 2.2\times 10^8$ rad/s.

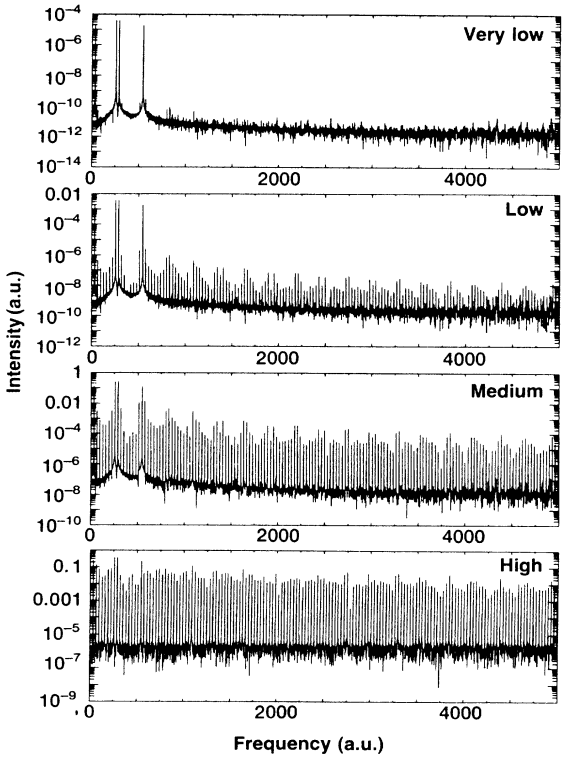

FIG. 6. Power spectrum of the intensity $I_3(\tau)$ for very low, low, medium, and high coupling strength for commensurate frequencies Δ_1 and Δ_2. The conversion to units of angular frequency is 1 arb. units $\leftrightarrow 2.2\times 10^8$ rad/s.

beams (even if the two input beams overlap well spatially). When one of the fields has large amplitude and the other has small amplitude, the photons in the large amplitude field are not converted (in SHG fields 1 and 2 are identical and therefore they are both simultaneously either large or small). Greatly improved SFG or DFG conversion efficiency with multifrequency laser beams can be achieved using an arrangement with two nonlinear mixing crystals, separated by a delay line for only one of the laser beams. This permits beam i to be delayed by a time L_i/c relative to the other beam. The time delay provides a relative shift of the modulated intensities of the beams, assuring an increased value of the second-order correlation function of the beams in the second crystal, thereby increasing the SFG conversion efficiency. The beams are then recombined by means of dichroic mirror and sent into the second mixing crystal. The output from both crystals can be combined by means of a polarization coupler. Studies demonstrating efficiency improvement will be presented elsewhere.

Summarizing, we find that 3WM of multifrequency input beams produces output with spectral bandwidth much larger than previously believed. In the high coupling strength limit, the output spectrum is limited only by the crystal phase-matching bandwidth. A new experimental technique for improving SFG and DFG conversion efficiencies was presented. Similar features occur whenever multifrequency beams propagate through nonlinear media, and therefore the concepts presented here are of relevance to nonlinear coupled systems in other fields of physics.

---

*Permanent address.

[1]N. Bloembergen, *Nonlinear Optics* (Benjamin, New York, 1965).

[2]J. A. Armstrong, N. Bloembergen, J. Ducing, and P. S. Pershan, Phys. Rev. **127**, 1918 (1962).

[3]Y. R. Shen, *The Principles of Nonlinear Optics* (Wiley, New York, 1984), pp. 67–140.

[4]A. A. Gusev, S. V. Kruzhalov, B. V. L'vov, L. N. Pakhomov, and Y. Yu, Petrun'kin, Kvant. Elektron. (Moscow) **10**, 547 (1983) [Sov. J. Quantum Electron. **13**, 322 (1983)] H. S. Kwok and P. H. Chiu, Opt. Lett. **10**, 28 (1985); C. J. Sun and J. T. Lue, IEEE J. Quantum Electron. **QE-24**, 113 (1988).

[5]*Handbook of Mathematical Functions,* Natl. Bur. Stand. Appl. Math. Ser. No. 55, edited by M. Abramowitz and J. A. Stegun (U.S. GPO, Washington, D.C., 1965), pp. 569–581.